Simulations of human movements through temporal discretization and optimization

by

Manindra Kaphle

November 2007
Licentiate Thesis from
Royal Institute of Technology
Department of Mechanics
SE-100 44 Stockholm, Sweden

Abstract

Study of physical phenomena by means of mathematical models is common in various branches of engineering and science. In biomechanics, modelling often involves studying human motion by treating the body as a mechanical system made of interconnected rigid links. Robotics deals with similar cases as robots are often designed to imitate human behaviour. Modelling human movements is a complicated task and, therefore, requires several simplifications and assumptions. Available computational resources often dictate the nature and the complexity of the models. In spite of all these factors, several meaningful results are still obtained from the simulations.

One common problem form encountered in real life is the movement between known initial and final states in a prespecified time. This presents a problem of dynamic redundancy as several different trajectories are possible to achieve the target state. Movements are mathematically described by differential equations. So modelling a movement involves solving these differential equations, along with optimization to find a cost effective trajectory and forces or moments required for this purpose.

In this study, an algorithm developed in Matlab is used to study dynamics of several common human movements. The main underlying idea is based upon temporal finite element discretization, together with optimization. The algorithm can deal with mechanical formulations of varying degrees of complexity and allows precise definitions of initial and target states and constraints. Optimization is carried out using different cost functions related to both kinematic and kinetic variables.

Simulations show that generally different optimization criteria give different results. To arrive on a definite conclusion on which criterion is superior over others it is necessary to include more detailed features in the models and incorporate more advanced anatomical and physiological knowledge. Nevertheless, the algorithm and the simplified models present a platform that can be built upon to study more complex and reliable models.

Key Words: Forward dynamics, Biomechanics, Temporal discretization, Optimization

Contents

CHAPTER 1

Introduction

1.1. Background

Study of physical phenomena by means of mathematical models is common in various branches of engineering and science. Biomechanics is one of such fields that has seen an increase in mathematical modelling studies, especially with the recent advances in computing resources. Biomechanics can be defined as the science that applies the principle of mechanics to biological systems, (Goldsmith 1996). It is a growing and important field and finds its applications in several areas.Modelling human movements is an important part of biomechanics. Results from modelling enhance the understanding behind the movements and improve the knowledge about the defects related to movements. Thus, biomechanical studies facilitate areas like diagnosis, surgery and prostheses, (Fung 1993). Another area of application of biomechanics is the field of sport mechanics. Studies on sporting activities can be expected to provide means of enhancing performance of athletes and understanding injury mechanisms in athletic activities.

Two approaches are commonly used for the study of human movements. The inverse dynamics approach involves measuring body segment kinematics, external forces and segment inertial characteristics and using them to compute joint moments and forces (Hamill and Selbie 2004). Position, velocity and acceleration data needed are usually obtained by optoelectronic methods which use special markers and sensors, (Lehman et al. 1996). The forward dynamics approach takes the opposite route, where known forces and torques are used to find the movement of the system. Mathematically, dynamic movements are described by differential equations, which are usually nonlinear in nature. In forward dynamics these differential equations are integrated forward in time (Nuzzo 2006). Inverse dynamics calculations are less expensive computationally than forward dynamics calculations, but the main drawback of inverse analysis is that it requires accurate measurements of external forces and body motions (Pandy 2001). Moreover, availability of improved computational power has made forward dynamics calculations reasonably efficient.

The human body is a complex structure and modelling its activities presents several challenges. For simplicity, the body parts are commonly modelled as rigid segments and the joints are treated as perfect hinges. Often it is necessary to restrict the movements in a certain plane, thus making them two dimensional in nature. Muscles are

ultimate actuators of movements and when included in models their behaviour is simplified. In spite of these simplifications several meaningful results can be obtained from modelling studies.

One common form of movement is where target control is desired. In such movement, along with the initial conditions, some or all of the final or target conditions are known. For such movement several different trajectories may be possible, thus giving rise to dynamic redundancy in trajectory selection. Optimization based on the parameters of the movement is a common way to determine how a trajectory is selected. Problems of this nature are frequently encountered in robotics in trajectory planning, which involves finding a trajectory that connects the initial and final configurations while satisfying other specified constraints at endpoints, such as velocity and acceleration constraints (Spong et al. 2006).

There is a vast range of literature dealing with human motion. Movements such as reaching, jumping and walking have been subjected to detailed analyses. Studies modelling dynamics of motion have usually incorporated three parts: 1) treatment of body parts as multi-link rigid segments, 2) treatment of muscles and tendons as actuators and 3) muscle activation dynamics to model delay in activation or relaxation of muscles, (Pandy et al. 1990; Pandy 2001; Stelzer and von Stryk 2003; Menegaldo et al. 2003). Walking/gait has been the subject of analysis of several different studies, (Onyshko and Winter 1980; Pandy and Berme 1988; Johansson and Magnusson 1991; Anderson and Pandy 2001; Kaplan and Heegaard 2001; Ren et al. 2007). Similarly, Pandy et al. (1990); Selbie and Caldwell (1996); Spägele et al. (1999) have investigated several features of high jump. Lots of studies have been carried out on trajectory planning in robotics with different settings and objectives, (Hargraves and Paris 1987; Enright and Conway 1991; Betts and Huffman 1992; Macfarlane and Croft 2003).

1.2. Aims and scope

In this study, forward dynamic models of several common human movements will be analyzed, using a method based on the temporal finite element discretization along with standard optimization tools, (Eriksson 2005, 2007). Activities are modelled as targeted movements and the actuating moments or forces needed to achieve the desired target state are identified as the ‘controls’. This study aims to investigate how a trajectory is selected by testing different optimization criteria based on the parameters of the movement. Optimization criteria tested are both kinematic and kinetic in nature. Kinematic criteria deal with parameters like displacement, velocity, acceleration and jerk (which measures smoothness of a movement) while kinetic ones deal with the controls.

Results of different optimization criteria are compared. Where possible, results from the simulations are compared to the results from other studies or natural movements. In addition to dynamic redundancy, biomechanical models also deal with static redundancy in the form of force distribution among muscles, (Dul et al. 1984; Stelzer and von Stryk 2003; Heintz and Gutierrez-Farewik 2007). Though most models in

this study are actuated by joint torques, attempts have been made to use muscles as actuators in some models. Muscle activation dynamics behind the force production in muscles is ignored, thereby assuming that the forces are regulated infinitely quickly. To summarize, the main objective of this study can be stated as testing the efficiency of the proposed numerical method and its suitability in studying of dynamics of biomechanical systems.

1.3. Outline of thesis

Chapter 2 discusses the numerical theory behind the work and a brief introduction to optimization methods. Chapter 3 deals with the biomechanical examples studied and the results obtained. Chapter 4 presents results from the simulations and these are subsequently discussed in Chapter 5. Conclusions from studies and the scope for future work are dealt with in Chapter 6.

CHAPTER 2

Numerical Methods

An algorithm is developed in Matlab (The MathWorks, Inc., Natick, MA, USA) to analyze forward dynamic models of human movements. It deals with two main areas of analysis: the treatment of structural dynamics by means of temporal discretization and optimization. Brief descriptions of the two areas and how their combination is used are presented in this chapter.

2.1. Temporal finite element

This section describes the temporal discretization method, which forms the basis for solving the models presented in the study. The method has similarities with work done by Kaplan and Heegaard (2001, 2002). It essentially involves converting differential equations into algebraic ones by dividing the total duration of a movement into a number of intervals. The values of state variables (displacements and velocities) and controls (for example, joint moments or muscle forces) at the discretized points are the unknowns which are solved for to determine the behaviour of the system.

For movements with prespecified target, several different possibilities exist for achieving that state from the initial one. Therefore, some measure of the control forces or of state variables is used as the cost function which is minimized to obtain the optimal trajectory. Several aspects of optimization are discussed in the next section. Alternates like shooting methods exist for solving boundary value differential equations but are deemed computationally expensive and unreliable for complex and large problems (Eriksson 2007).

The main formulation underlying the algorithm has been stated in Eriksson (2005, 2007). A general description of the formulation is presented here.

2.1.1. *Description of movement*

For a system with N_d degrees of freedom, the configuration at time t is described by a set of N_d displacement coordinates $q_i(t)$, collected in:

$$\boldsymbol{q}(t) = \begin{pmatrix} q_1(t) \\ q_2(t) \\ \vdots \\ q_{N_d}(t) \end{pmatrix} \tag{2.1}$$

for a time interval $0 \leq t \leq T$.

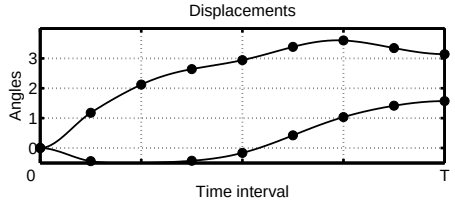

Figure 2.1: Example of interpolation of displacement coordinates from their values and time differentials at chosen time stations. At each time station, both value and its time differential are known, leading to a locally cubic curve.

In order to capture a dynamic movement, the velocities in the used coordinate directions are included, and the configuration is thereby described by a vector of double size:

$$\boldsymbol{Q}(t) = \begin{pmatrix} q_1(t) \\ \dot{q}_1(t) \\ q_2(t) \\ \vdots \\ \dot{q}_{N_d}(t) \end{pmatrix} \tag{2.2}$$

with the superposed dots representing the time differential.

The studied time interval is divided into $N_t + 1$ equally spaced time stations:

$$t^j = j \cdot \frac{T}{N_t} \tag{2.3}$$

for ($0 \leq j \leq N_t$). At each discrete time station, the configuration is thus specified by the degrees of freedom:

$$\boldsymbol{Q}^j = \boldsymbol{Q}(t^j) \equiv \left(q_1(t^j), \dot{q}_1(t^j), q_2(t^j), \ldots, \dot{q}_{N_d}(t^j)\right)^{\mathrm{T}} \tag{2.4}$$

The initial state is specified by the configuration $\boldsymbol{Q}(0)$. A target configuration can be specified by $\boldsymbol{Q}(\theta)$, where θ is often equal to T, although the algorithm allows specification of intermediate target states. A target configuration need not necessarily specify all displacement and velocity components.

The whole movement is described by the collection of values at all time stations:

$$\boldsymbol{Q} = \left[(\boldsymbol{Q}^0)^{\mathrm{T}}, (\boldsymbol{Q}^1)^{\mathrm{T}}, (\boldsymbol{Q}^2)^{\mathrm{T}}, \ldots, (\boldsymbol{Q}^{N_t})^{\mathrm{T}}\right]^{\mathrm{T}} \tag{2.5}$$

which is a vector of length $2\,N_d(N_t + 1)$.

A Hermitian interpolation is used in the algorithm for the description of a coordinate value at any point within the interval, Fig. 2.1.

The basic interpolation of one coordinate can be written as:

$$q_i(t) = N_1(t)q_i^j + N_2(t)\dot{q}_i^j + N_3(t)q_i^{j+1} + N_4(t)\dot{q}_i^{j+1} \qquad \text{for} \qquad t^j \leq t \leq t^{j+1} \tag{2.6}$$

where N_1, N_2, N_3 and N_4 are the local shape functions, (Cook et al. 2002).

The coordinates at time t, $\boldsymbol{q}(t)$, can thereby be collected as:

$$\boldsymbol{q}(t) = [\mathbb{N}(t)]\,\boldsymbol{Q} \tag{2.7}$$

where the matrix $\mathbb{N}(t)$ is of size $(N_d) \times 2N_d(N_t + 1)$, but is sparse as only a few functions are non-zero at time t, (Zienkiewicz and Taylor 2000). The description gives C^1 time continuity over time element borders.

The velocity and acceleration components are consistently described as:

$$\boldsymbol{v}(t) \equiv \dot{\boldsymbol{q}}(t) = \left[\dot{\mathbb{N}}(t)\right]\boldsymbol{Q} \tag{2.8}$$

$$\boldsymbol{a}(t) \equiv \ddot{\boldsymbol{q}}(t) = \left[\ddot{\mathbb{N}}(t)\right]\boldsymbol{Q} \tag{2.9}$$

2.1.2. *Controls*

In addition to internal forces related to the current configuration, two groups of external forces were considered. The first group consists of gravity and applied forces, with known time variations. Displacement independent external forces are a priori defined as $\boldsymbol{p}(t)$. The algorithm also allows a set of N_c a priori unknown controls, $c_i(t)$ $(1 \leq i \leq N_c)$. At time t, the acting controls are collected as:

$$\boldsymbol{c}(t) = \begin{pmatrix} c_1(t) \\ c_2(t) \\ \vdots \\ c_{N_c}(t) \end{pmatrix} \tag{2.10}$$

The controls are discretized at N_k time stations τ^j,

$$\boldsymbol{C}^j = \boldsymbol{c}(\tau^j) = \left(c_1(\tau^j), c_2(\tau^j), \ldots, c_{N_c}(\tau^j)\right)^{\mathrm{T}} \tag{2.11}$$

with $0 \leq \tau^j \leq T$, and $1 \leq j \leq N_k$, preferrably coinciding with a subset of the displacement time stations. The whole set of unknown control components is collected as:

$$\boldsymbol{C} = \left[(\boldsymbol{C}^1)^{\mathrm{T}}, (\boldsymbol{C}^2)^{\mathrm{T}}, \ldots, (\boldsymbol{C}^{N_k})^{\mathrm{T}}\right]^{\mathrm{T}} \tag{2.12}$$

A linear interpolation is used in the algorithm for the controls, Fig. 2.2. For a specific time instance t:

$$\boldsymbol{c}(t) = [\mathbb{N}_c(t)]\,\boldsymbol{C} \tag{2.13}$$

where the matrix $\mathbb{N}_c(t)$ is $N_c \times (N_c N_k)$, but very sparse: at most two values in each row are non-zero.

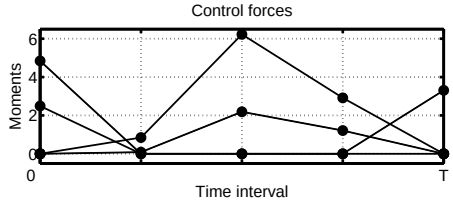

Figure 2.2: Example of interpolation of control forces from their values at chosen time stations. At each time station only the value is known, leading to a locally linear representation.

Controls can be of different nature. For example, in case of rotational movement joint torques can be used as controls. Similarly, in a biomechanical model muscle forces or muscle tensions may be used as controls. In the latter case, the muscle actuators are often a redundant set for creating the joint torques.

2.1.3. *Mechanical equilibrium equations*

The dynamical system is governed by $N_e \equiv N_d$ equilibrium equations, which can be stated for a specific time instance t as, (Eriksson 2005):

$$\mathbf{M}\boldsymbol{a}(t) + \boldsymbol{f}(\boldsymbol{q}(t), \boldsymbol{v}(t)) - \boldsymbol{p}(t) - \mathbf{E}_c\boldsymbol{c}(t) = \mathbf{0} \tag{2.14}$$

where $\mathbf{M}$ is the mass matrix and $\boldsymbol{q}(t)$, $\boldsymbol{v}(t)$ and $\boldsymbol{a}(t)$ are the displacements, velocities and accelerations, respectively. The vector $\boldsymbol{f}$ describes all internal forces and displacement affected loads. In linear case, $\boldsymbol{f}(\boldsymbol{q}(t), \boldsymbol{v}(t)) = [\boldsymbol{K}]\boldsymbol{q}(t) + [\boldsymbol{D}]\boldsymbol{v}(t)$, where $[\boldsymbol{K}]$ and $[\boldsymbol{D}]$ represent the stiffness and damping matrices respectively. $\boldsymbol{p}(t)$ denotes the external forces acting in the system. The effects of controls $\boldsymbol{c}(t)$ are described by an action description matrix $\mathbf{E}_c$, of size $N_d \times N_c$.

With these values, a time instance residual form is written:

$$\boldsymbol{e}(t) \equiv \boldsymbol{e}(\boldsymbol{q}(t), \boldsymbol{v}(t), \boldsymbol{a}(t), \boldsymbol{p}(t), \boldsymbol{c}(t); t) = \mathbf{0} \tag{2.15}$$

where the equations must be formally derived for a specific structural system, by any method, general enough for the problem context, (Calkin 1996; Knudsen and Hjorth 1996).

The N_d equilibrium equations given by Eq. (2.15) are demanded to be fulfilled at $2 \cdot N_t$ collocation points over the total interval resulting in a set of $2N_dN_t$ equations, cf. (Kaplan and Heegaard 2002). The resulting equations can be seen as

$$\boldsymbol{E}(\boldsymbol{Q}, \boldsymbol{C}, \boldsymbol{P}) = \mathbf{0} \tag{2.16}$$

with $\boldsymbol{P}$ representing the external forces $\boldsymbol{p}(t)$ for all time stations.

The choice of collocation points within each interval is arbitary; in this study, two Gauss quadrature points are used as the collocation points within each of the N_t time intervals (Eriksson 2005, 2007).

2.1.3.1. *Boundary values and restrictions*

A set of N_b linear equality conditions on the discrete coordinates are introduced by:

$$\boldsymbol{B}(\boldsymbol{Q}) \equiv \mathbf{B}_Q \, \boldsymbol{Q} - \boldsymbol{b}_Q = \mathbf{0} \tag{2.17}$$

At least $2N_d$ conditions are needed to define an initial state at $t = 0$. Excessive boundary conditions define a target state, and imply the need for at least $N_c N_k = N_b - 2N_d$ free control force components.

The movement of a system can be mechanically or physiologically restricted. Simple kinematic restrictions can often be seen as linear inequalities in the coordinates as:

$$\mathbf{B}_R \boldsymbol{Q} - \boldsymbol{b}_R \leq \mathbf{0} \tag{2.18}$$

As the restrictions are valid at all time stations, the number of restrictions becomes high.

The unknown controls might also be kinetically restricted. This demands, when all control force time stations are collected:

$$\mathbf{B}_L \boldsymbol{C} - \boldsymbol{b}_L \leq \mathbf{0} \tag{2.19}$$

For further treatment, Eqs. (2.18) and (2.19) can be collected as:

$$\mathbf{B}_G \begin{pmatrix} \boldsymbol{Q} \\ \boldsymbol{C} \end{pmatrix} - \boldsymbol{b}_G \leq \mathbf{0} \tag{2.20}$$

2.2. Optimality of movement

When excessive control force components are present, an optimal solution can be sought. This involves defining a 'cost' or 'performance' function which is then minimized to obtain the best possible solution. The cost functions can be kinetic, kinematic or combined in nature. Kinetic cost functions measure the costs on the control forces needed to produce the desired motion. For instance, an integrated sum of squared control forces over the considered time interval gives a cost function:

$$\Pi_{cc} \equiv \frac{1}{2} \int_0^{\mathrm{T}} \left(\sum_i \left(c_i(t) \right)^2 \right) dt = \sum_i \sum_j \Pi_i^j = \boldsymbol{C}^{\mathrm{T}} \mathbb{C}_{cc} \boldsymbol{C} \tag{2.21}$$

with simple form for the matrix $\mathbb{C}_{cc}$, (Eriksson 2005). This form is easily algorithmically handled, although a more natural measure for the needed force is a weighted average control force norm:

$$\|\boldsymbol{c}\|_T = \sqrt{\frac{2}{T} \Pi_{cc}} \tag{2.22}$$

Another cost function proposed by Uno et al. (1989) measures the cost of rate of change of control forces and can be stated as:

$$\Pi_{ct} \equiv \frac{1}{2}\int_0^{\mathrm{T}} \left(\sum_i \left(\frac{dc_i}{dt} \right)^2 \right) dt = \boldsymbol{C}^{\mathrm{T}} \mathbb{C}_{ct} \boldsymbol{C} \tag{2.23}$$

Kinematic cost functions measure the cost on the state variables, rather than the control forces. Seeking an optimally smooth movement, a jerk cost can be formulated, based on the idea by Flash and Hogan (1985). Jerk components are the third time differentials of the displacements (constants in each interval) and can be written as:

$$\boldsymbol{j}(t) \equiv \dddot{\boldsymbol{q}}(t) = [\dddot{\mathbb{N}}(t)]\, \boldsymbol{Q} \tag{2.24}$$

A cost expression for the integrated sum of squared jerk components can thus be stated as:

$$\Pi_{qj} \equiv \frac{1}{2}\int_0^{\mathrm{T}} \left(\sum_i \left(j_i(t) \right)^2 \right) dt = \boldsymbol{Q}^{\mathrm{T}} \mathbb{C}_{qj} \boldsymbol{Q} \tag{2.25}$$

Similarly, a cost for accelerations and velocities can be defined as:

$$\Pi_{qa} \equiv \frac{1}{2}\int_0^{\mathrm{T}} \left(\sum_i \left(a_i(t) \right)^2 \right) dt = \boldsymbol{Q}^{\mathrm{T}} \mathbb{C}_{qa} \boldsymbol{Q} \tag{2.26}$$

$$\Pi_{qv} \equiv \frac{1}{2}\int_0^{\mathrm{T}} \left(\sum_i \left(v_i(t) \right)^2 \right) dt = \boldsymbol{Q}^{\mathrm{T}} \mathbb{C}_{qv} \boldsymbol{Q} \tag{2.27}$$

Based on the formulations above, the studied constrained optimization problem can be stated as:

$$\begin{aligned} \text{mimimize} \quad & \Pi_z \equiv \Pi(\boldsymbol{z}) \\ \text{under equality constraints} \quad & \boldsymbol{b}_1(\boldsymbol{z}) = 0 \\ \text{and inequalities} \quad & \boldsymbol{b}_2(\boldsymbol{z}) \leq 0 \end{aligned} \tag{2.28}$$

In the developed form, the unknown $\boldsymbol{z}$ contains both the state variables and the control forces:

$$\boldsymbol{z} = \begin{pmatrix} \boldsymbol{Q} \\ \boldsymbol{C} \end{pmatrix} \tag{2.29}$$

and the cost function is based on these variables. Allowing any of the cost functions discussed above, it can be written as:

$$\Pi(\boldsymbol{z}) \equiv \Pi(\boldsymbol{Q}, \boldsymbol{C}) = \alpha_c \boldsymbol{C}^{\mathrm{T}} \mathbb{C}_{\mathbf{c}} \boldsymbol{C} + \alpha_q \boldsymbol{Q}^{\mathrm{T}} \mathbb{C}_{\mathbf{q}} \boldsymbol{Q} \tag{2.30}$$

where

$$\alpha_c \mathbb{C}_{\mathbf{c}} = \alpha_{cc} \mathbb{C}_{\mathbf{cc}} + \alpha_{ct} \mathbb{C}_{\mathbf{ct}} \tag{2.31}$$

$$\alpha_q \mathbb{C}_{\mathbf{q}} = \alpha_{qj} \mathbb{C}_{\mathbf{qj}} + \alpha_{qa} \mathbb{C}_{\mathbf{qa}} + \alpha_{qv} \mathbb{C}_{\mathbf{qv}} \tag{2.32}$$

and the α coefficients choose the criterion for the minimization.

The equality constraints $\boldsymbol{b}_1(\boldsymbol{z}) = 0$ include a non-linear part corresponding to the set of equilibrium equations, Eq. (2.16) and a linear part representing the boundary conditions, Eq. (2.17). The inequality constraints $\boldsymbol{b}_2(\boldsymbol{z}) \leq 0$ represent the restrictions according to Eq. (2.20).

2.3. Algorithmic implementation

An algorithm is developed in Matlab that encompasses both aspects of numerical methods discussed above. The function 'fmincon' included in the 'Optimization toolbox' of Matlab offers a suitable format for solving the stated problem. Fmincon solves nonlinear optimization problems by using sequential quadratic programming (SQP). SQP is a popular technique for solving a nonlinearly constrained problem. A brief discussion of SQP is provided in Appendix A.

Several other computational packages are available for constrained nonlinear optimization. An important aspect for any algorithm is the size of the problem, which often involves hundreds of variables and large numbers of equality and inequality constraints. The formulation is, however, extremely sparse for large problems. This fact has only been exploited to a limited degree, but could allow significant improvements in efficiency, (Beauwens 2004).

The algorithm takes as its basis a sufficiently complete mechanical formulation of dynamics of a system. A convenient way to derive the dynamic equations is through the Euler-Lagrange method, considering kinetic energies of the segments and potential energies of all the loads, (Calkin 1996; Knudsen and Hjorth 1996; Winter 2005).

The developed algorithm consists of interaction of two main parts: a central component 'Optcon' and a definition file specifying problem specific details. Optcon is a common platform for all problems, while seperate definition files are needed for different models. The working of the algorithm is summarized in Fig. 2.3.

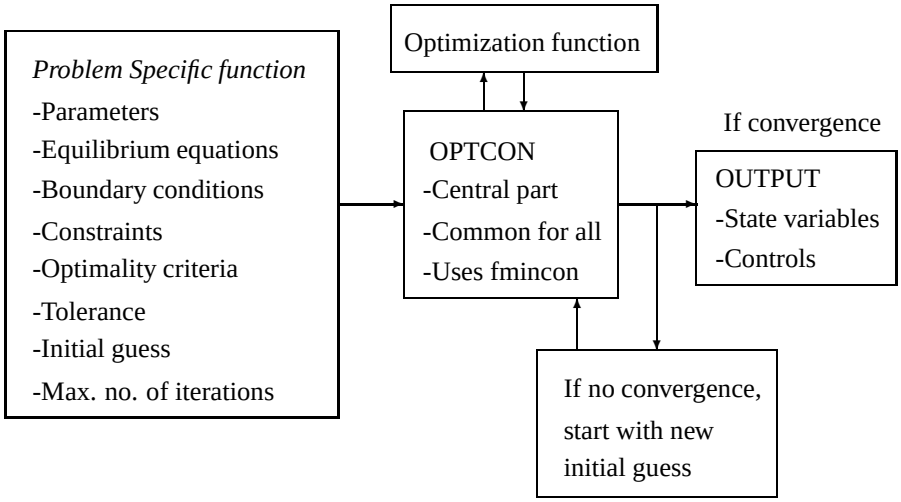

Figure 2.3: Summary of the developed algorithm

Optcon uses the Matlab function fmincon for optimization calculations. Parameters of the model, equilibrium equations, boundary conditions, constraints, optimality criteria and the maximum number of allowable iterations are all supplied in a definition file. To speed up the calculations gradients of the equilibrium equations and constraints are required. These are obtained by differentiation of the equations by the variables. Symbolic differentiation is easily carried out by packages like Mathematica, (Wolfram Research, Inc., Champaign, IL., USA) and Maple (Maplesoft, Waterloo Maple Inc, Canada).

An initial guess of the solution is needed to start the iterations and is supplied in the problem definition file. Fmincon can even start calculation from an unfeasible solution. But, as the complexity of the system rises, the specification of a suitable initial guess can be troublesome. One method used was to obtain a solution with larger value of tolerance and use this solution to obtain a solution with lower tolerance, and repeat this process till a solution with desired amount of tolerance is obtained. It is also possible for the solution to be attracted to a local optimum instead of a global optimum and it is hard to ascertain whether a solution is globally or locally optimal. One possible remedy is to start with different initial guesses and to see if they all converge to the same solution; and if they do not, then pick the solution with the smallest cost.

Optcon also interacts with another component that supplies the desired optimization function and its gradients, depending on the optimality criteria specified in the definition file. It is noted that the quadratic nature of the cost functions, cf. Eqs. 2.21, 2.23, 2.25 – 2.27 , enables easier differentiation. A fairly small value of tolerance is supplied and the iterations run till this tolerance is met in the function value and constraints. On succesful completion of optimization, state variables (displacements and velocities) and controls are provided as the outputs. If no convergence is obtained within the provided number of iterations, an error message is displayed.

Thus, specification of the modelling process is manual and leaves options for further development for more automatic implementation. User friendly interface by means of interaction with other softwares like the musculoskeletal modelling package SIMM (Musculographics Inc., Santa Rosa, CA) and Sophia (Lesser 1995) is possible. Efficient plotting and visualizing of the results can be another important improvement in the algorithm.

CHAPTER 3

Examples

Some common day to day activities are analysed next. The initial studies deal with simple upper limb movement in vertical and horizontal planes. More complex activities like jumping, stepping and weightlifting are also investigated. The movements studied are of targeted control types, commonly associated with robotics. Initial conditions (positions and velocities) and all or some of the final conditions are assumed to be known. Intermediate states, if known, can be easily introduced too. The duration of movement is always known.

As discussed earlier, redundancy exists in choosing paths during a certain motion. How a certain trajectory is selected as the chosen human movement is not completely understood. Several approaches have been assumed to guide the choice, for example, minimization of smoothness of the trajectory, minimization of the joint torques or minimization of the joint torque changes.

3.1. Movement of upper limb in the sagittal plane

The first example studied was the movement of upper limb in a sagittal plane. The model consisted of two interconnected rigid links representing the upper and the lower arm segments, as seen in Fig. 3.1. The arm configuration was described by two joint angles, the elbow flexion angle q_1 and the shoulder flexion angle q_2, Fig. 3.1b.

Anatomical data for the model were chosen as $L_1 = 0.32$ m, $L_2 = 0.25$ m, with gravity forces $g_1 = 11$ N, $g_2 = 20$ N, $g_3 = 5$ N, based on anthropometrical data of a 50^{th} percentile male, Winter (2005); the weights g_1 and g_2 were assumed to act in the centers of the segments, the hand weight g_3 at the wrist joint. The external carried load was assumed as $p_1 = 10$ N at the wrist.

The first problem analysed was the movement of the arm from a vertical hanging position $(q_1, q_2) = (0, 0)$ to a horizontal straight position $(q_1, q_2) = (0, \frac{\pi}{2})$ in a time period of $T = 0.5$ s. The velocities and the accelerations at the initial and final time instances were all zero. In order to carry out this movement, two control torques c_1 and c_2 were required at the elbow and shoulder joints respectively. T was divided into $N_t = 32$ equal parts for discretization of the state coordinates. The controls c_1 and c_2 were discretized at $N_k = 33$ time stations, including the initial and final times.

Moment arm data for the major upper limb muscles were obtained from a model developed by Holzbaur et al. (2005) for use in the commercially available musculoskeletal modeling software SIMM, (Musculographics Inc., Santa Rosa, CA), cf. Delp and

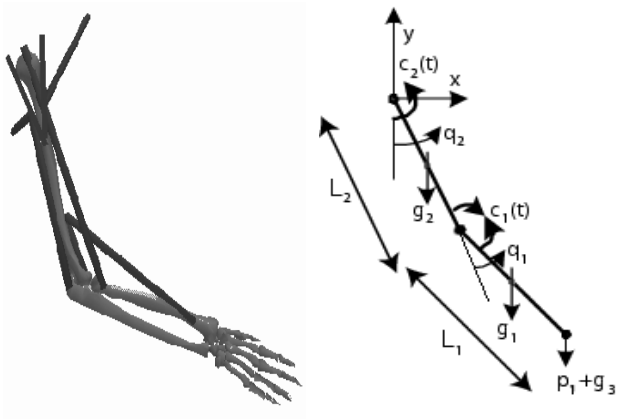

(a) (b)

Figure 3.1: Problem definition: a) musculoskeletal system; b) measures, coordinates, loads, and resultant moment at joints.

Loan (1995). Moment arm is the shortest distance between the line of action of muscle force and the joint's centre of rotation, where it is assumed that the force is constant along the whole muscle length. Muscle physiological cross sectional area (PCSA) data were obtained from Holzbaur et al. (2005).

Relevant data for the eight muscles were derived by Heintz et al. (2006). The moment arms (MA1, MA2) and the PCSA values were used to evaluate maximum and minimum joint control moment contributions, based on an assumed maximum muscle tension of $330\,\text{kPa}$, (Garner and Pandy 2001). Used data are given in Table 3.1, with muscle notation from Holzbaur et al. (2005)[1].

Summing the negative and positive components of the resultant moment contributions at the joints, see Table 3.1, restrictions were placed on c_1 and c_2 as follows:

$$-3.98 \leq c_1(t) \leq 13.0 \tag{3.1}$$

$$-7.65 \leq c_2(t) \leq 5.69 \tag{3.2}$$

where the values are given in Nm.

[1] The abbreviated muscle names refer to: *Biceps long head, Brachialis, Brachioradialis, Triceps long head, Deltoid (Ant., Post.), Pectoralis major clavicular, and Latissimus dorsi thoraic.*

Table 3.1: Used muscle data. Moment arm MA1 is at elbow and MA2 at shoulder, positive for flexion, negative for extension. Muscular area PCSA is physiological cross sectional area. Max-M1 and Max-M2 are limits for contributions to resultant moments at the joints. Notation and PCSA data from a SIMM model based on Holzbaur et al. (2005).

Muscle	MA1 $[10^{-3}\text{m}]$	MA2 $[10^{-3}\text{m}]$	PCSA $[10^{-4}\text{m}^2]$	Max-M1 [Nm]	Max-M2 [Nm]
BICL	35.6	7.06	4.50	5.28	1.05
BRA	17.6	0	7.10	4.12	0
BRD	57.3	0	1.90	3.60	0
TRIL	-21.2	-20.3	5.70	-3.98	-3.82
DELT1	0	17.2	8.20	0	4.64
DELT3	0	-8.21	1.90	0	-0.52
PMAJ1	0	-5.83	2.60	0	-0.50
LAT1	0	-30.4	2.80	0	-2.81

To prevent excessive elbow flexion, restrictions were put on the elbow angle q_1 as follows:

$$0 \leq q_1(t) \leq \frac{3\,\pi}{4} \tag{3.3}$$

No restrictions were put on the shoulder angle q_2.

Simulations were performed with respect to the five criteria discussed in Section 2.2. For scaling reasons, the cost functions were evaluated with either of $\alpha_{cc} = 1$, $\alpha_{ct} = 1 \cdot 10^{-4}$, $\alpha_{qv} = 1 \cdot 10^{-2}$, $\alpha_{qa} = 1 \cdot 10^{-4}$ or $\alpha_{qj} = 1 \cdot 10^{-6}$, the others being zero; the obtained results are denoted by the non-zero coefficient.

For obtained solutions, the five cost functions in Eqs. (2.21, 2.23, 2.25 – 2.27) were evaluated. The similarities among the results obtained from five different cost criteria were evaluated by calculating colinearity between displacement states Q_i and Q_j as:

$$\gamma_{ij} = \frac{Q_i^T \cdot Q_j}{\parallel Q_i \parallel \cdot \parallel Q_j \parallel} \tag{3.4}$$

Further simulations were performed varying the total duration of the movement. For these, $\alpha_{cc} = 1$ was used and variation in force cost was studied.

The basic case in this example used values of N_t and N_k such that $N_k - 1 = N_t$, implying that state variables and the controls were discretized into the same numbers of intervals. To study the effects of the values of N_t and N_k, next set of simulations was performed with N_t kept constant at 16 while using three values values (17,21,33) for N_k.

3.2. Tensions in muscles

In vivo measurement of muscle forces can be done only by invasive techniques like the use of tendon transducers (Lehman et al. 1996). Such experiments are not easy to carry out due to ethical and practical reasons. Calculating these forces by computer simulations is an interesting alternative. The next set of simulations was aimed at determining tensions in muscles during the upper limb movement.

Control torques at each joint can be calculated first as done in the previous section, followed by force distribution among the involved muscles using static optimization at each time instance, (Heintz et al. 2006; Heintz and Gutierrez-Farewik 2007). Another option is to carry out these two issues simultaneously. For this, eight muscle tensions instead of two joint torques were chosen as controls in optimization. A maximum muscle tension of 400 kPa for each muscle was used as restriction, as no convergence was obtained with the lower values. Though moment arms of muscles change with orientation, averaged values were used.

Two cost criteria (minimum control forces and minimum control force changes) were used. Jerk criterion was omitted as it did not involve control forces directly in calculations, and thereby produced random distribution among fully synergistic muscles, unless a small value of other criterion, such as α_{cc} was used together with $\alpha_{qj} \neq 0$.

3.3. Movement of upper arm in the horizontal plane

Several studies in the past have studied the upper limb movement in the horizontal plane, (Morasso 1981; Abend et al. 1982; Flash and Hogan 1985; Uno et al. 1989). These experiments on point to point targeted arm movement have demonstrated straight or slightly curved arm trajectories with bell shaped tangential velocity profile, (Flash and Hogan 1985; Uno et al. 1989).

The dynamic equations and settings were similar to those in the sagittal plane, but without gravitational effects and external forces. No restrictions were introduced for moments, while a restriction was introduced in the elbow angle to prevent hyperextension, $0 \leq q_1$. Simulations were performed for two different movements in the horizontal plane. The first case involved a movement between two states located approximately in front of the body, while the second one included larger movements. Similar movements were analysed in Uno et al. (1989) and Ohta et al. (2004).

Results from the simulations were compared with those from literature to observe which optimality cost function gave the best matching results.

3.4. High jump

High jump has been a subject of investigation of several studies, (Pandy et al. 1990; Selbie and Caldwell 1996; Spägele et al. 1999). A four link model was used to simulate high jumping, see Figure 3.2. The links represented foot, shank, thigh and upper

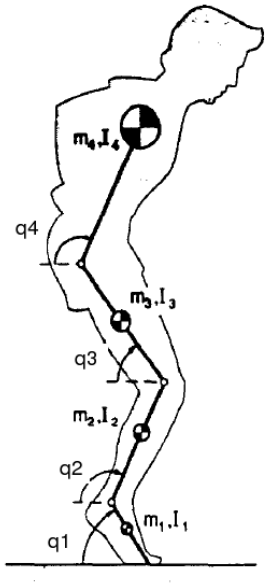

Figure 3.2: High jump model, reproduced from Pandy et al. (1990)

Table 3.2: Parameters related to high jump model

Segments	Length (m)	Mass (kg)	I (kgm^2)
Foot	0.175	2.2	0.008
Shank	0.435	7.5	0.065
Thigh	0.400	15.15	0.126
HAT	0.343	51.22	6.814

body. All the motions were restricted in the sagittal plane. The four degrees of freedom q_1, q_2, q_3 and q_4 represented the angles the segments made with the horizontal. Equations and relevant data were obtained from Pandy et al. (1990)

Table 3.2 shows the parameters of the model. Mass moments of inertia (I) are given about the centres of the mass of the segments.

The initial part of jumping is the phase between the heel lift-off and the body lift-off and this phase was analysed. The jump started from a crouching position and all the segments except the foot were vertical when the lift-off took place. Boundary conditions specified are shown in Table 3.3. Jump was simulated for two different durations of $T = 0.2$ s and $T = 0.4$ s. Simulations were run using $\alpha_{ct} = 1$. With the values of velocities of the segments at the lift-off, the heights of the jump were calculated.

Table 3.3: Specified initial and final values for high jump model

		Initial ($t = 0$)	Final ($t = T$)
q_1	[°]	34	60
$\dot{q}_1$	[rad/s]	0	
q_2	[°]	120	90
$\dot{q}_2$	[rad/s]	0	
q_3	[°]	30	90
$\dot{q}_3$	[rad/s]	0	
q_4	[°]	120	90
$\dot{q}_4$	[rad/s]	0	

Table 3.4: Lower leg muscles

	Muscle	Function	Average MA (m)	PCSA (cm^2)
1)	Ilipsoas	Hip flexion	0.0276	16.0
2)	Rectus femoris	Hip flexion	0.4040	12.5
		Knee extension	−0.4026	
3)	Glutei	Hip extension	−0.0167	60.7
4)	Hamstring	Hip extension	−0.0473	30.0
		Knee flexion	0.0390	
5)	Vasti	Knee extension	−0.0392	27.0
6)	Gastrocnemius	Knee flexion	0.0156	30.0
		Ankle plantarflexion	−0.0402	
7)	Tibialis Anterior	Ankle dorsiflexion	0.0397	9.1
8)	Soleus	Ankle plantarflexion	−0.0396	58.0

In order to model the foot-ground interaction in Pandy et al. (1990), a damped torsional spring is used at the toes that applies moment, thereby keeping the foot segment above the ground. Here this was done by preventing the foot angle from being less than than the initial value of 34^o, that is, by introducing a restraint of the form $q_1(t) \geq 34^o$ during the whole duration of movement.

Eight major muscle groups are responsible for human lower limb movements, (Ackermann and Schiehlen 2006). The muscles along with some of their properties (average moment arms (MA) and PCSA) are listed in Table 3.4.

Average moment arm data were obtained from SIMM, and other muscle properties like PCSA from Winter (2005). Positive values denote flexion while negative denote extension.

3.5. Walking/Stepping

Walking is one of the common human movements and has been a subject of analysis of several different studies, (Onyshko and Winter 1980; Pandy and Berme 1988; Johansson and Magnusson 1991; Piazza and Delp 1996; Anderson and Pandy 2001; Kaplan and Heegaard 2001; Ren et al. 2007). Walking/gait disorders are common. Modelling provides information about joint torques and muscle forces and the knowledge of these is useful in further understanding of the mechanism of gait and in treatment of disorders. Movements similar to walking occur during other activities like stepping and stair climbing. Stepping is analyzed in several studies (Flashner et al. 1987; Chou and Draganich 1997; Armand et al. 1998; Chen and Lu 2006).

Figure 3.3 shows various stages of the gait cycle. The cycle consists of two primary stages: Stance phase comprising of about 60 % and swing phase comprising of the 40 % of the total cycle, (Sutherland et al. 1994). Before the swing phase there is double support phase which lasts about 10 % of the whole gait cycle. In double support phase both feet are on the ground simultaneously, and the swing leg undergoes toe-off at the end. In order to reduce computational cost, the gait cycle can be assumed to be bilaterally symmetrical and only 50 % of the cycle need to be analyzed, (Anderson and Pandy 2001). A full gait cycle forms one stride and each stride is made of two steps, thus a step forming 50 % of the gait cycle.

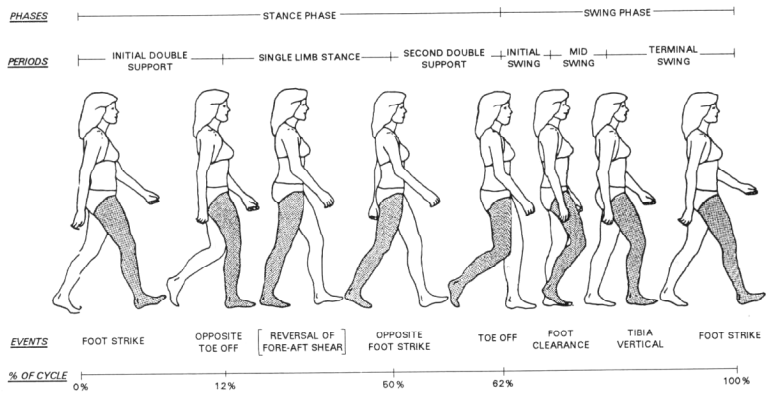

Figure 3.3: Various stages of gait cycle, reproduced from Sutherland et al. (1994)

A simple dynamic model is created to run gait simulations, similar to the one used by Armand et al. (1998) to analyze stepping. Complicated models are avoided because of higher computational cost involved. The model consists of four segments. Stance leg is kept straight and is represented by only one segment, while swing leg has three segments representing the stance leg and the swing femur, shank and foot. The four degrees of freedom, q_1, q_2, q_3 and q_4, represent the angle made by the stance leg with the ground and the angles at the hip, knee and ankle joints of the swing

Table 3.5: Parameters related to gait model

Segments	Length (m)	Mass (kg)	I (kgm^2)
Stance leg	0.6191	5.796	1.1141
Swing thigh	0.2698	3.60	0.0273
Swing shank	0.3493	1.674	0.0186
Swing foot	0.0554	0.522	0.0003

leg respectively, Figure 3.4. Anatomical data and other relevant data were obtained from Winter (2005). The model takes into account movements in the sagittal plane only.

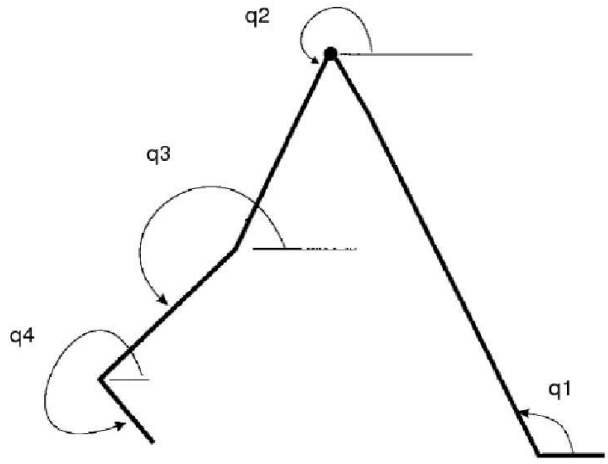

Figure 3.4: Walking model, reproduced from Armand et al. (1998)

Parameters related to the model are shown in Table 3.5, where Is denote the moment of inertias of the segments at the centre of mass, except for the stance leg where it is the moment of inertia around the ankle. Initial and final values for state variables were obtained from Gutierrez (2003). These are shown in Table 3.6.

The duration of movement was 0.47 s, which was equal to half of the averaged total duration for one gait cycle in the experiments. For temporal discretization, $N_t = 32$ and $N_k = 33$ were used. Restrictions were put on the state variables to prevent physiologically impossible states. One such case of knee hyperextension was avoided with restriction:

Table 3.6: Initial and final values for gait model

		Initial ($t = 0$)	Final ($t = T$)
q_1	[rad]	1.83	1.03
$\dot{q}_1$	[rad/s]	-2.00	-3.00
q_2	[rad]	4.52	5.32
$\dot{q}_2$	[rad/s]	0	0.65
q_3	[rad]	4.32	5.20
$\dot{q}_3$	[rad/s]	-3.53	0.52
q_4	[rad]	6.07	6.80
$\dot{q}_4$	[rad/s]	-6.53	0.55

$$q_3(t) - q_2(t) \leq 0 \tag{3.5}$$

Amounts of ankle dorsi- and plantarflexion more than $15^{\text{o}} = \pi/12$ were also prevented as:

$$q_4(t) - q_3(t) \geq 5\pi/12 \tag{3.6}$$

$$q_4(t) - q_3(t) \leq 7\pi/12 \tag{3.7}$$

To handle the double support phase at the start of the cycle, additional nonlinear constraints were introduced to constrain the toe position of the swing leg for the first 4 out of 32 total time stations. Equality constraints created some numerical problems, so instead two nonlinear inequality constraints were given; thus allowing toe position to vary by a very small amount (10^{-5}m).

3.6. Weightlifting

Lifting of a weight is a common activity and has been analyzed in several studies, (Chaffin and Andersson 1991; Hsiang et al. 1999; Chang et al. 2001). Weighlifting is also a popular sport and a common action involves lifting of the barbell from ground to about neck height in a single movement. Similar movement is also frequently encountered in robotics, where robots are designed to perform tasks such as lifting and moving goods from one position to another. Chang et al. (2001) used minimization of joint torques as criterion to analyse the lifting movement and compare the results with experimental studies.

A five segment model was used to simulate weightlifting, Figure 3.5. The five links represent the shank, thigh, body, upper arm and lower arm. Angles made by these segments with horizontal are denoted by q_1, q_2, q_3, q_4 and q_5.

The total duration $T = 1$s was discretized as $N_t = 32$ and $N_k = 33$.

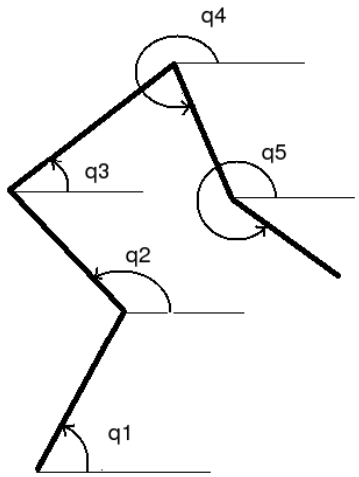

Figure 3.5: Weightlifting model

Table 3.7: Parameters related to weightlifting model

Segments	Length (m)	Mass (kg)	I (kgm^2)
Shank	0.431	4.27	0.1369
Thigh	0.428	7.00	0.1342
Body	0.504	47.50	9.8302
Upper arm	0.326	1.96	0.0215
Lower arm	0.256	1.54	0.0220

Table 3.8: Specified initial and final values for weightlifting model

		Initial ($t = 0$)	Final ($t = T$)
q_1	[rad]	0.8727	1.3090
$\dot{q}_1$	[rad/s]	0	
q_2	[rad]	2.6180	1.5708
$\dot{q}_2$	[rad/s]	0	
q_3	[rad]	0.3491	1.7453
$\dot{q}_3$	[rad/s]	0	
q_4	[rad]	4.8869	5.2360
$\dot{q}_4$	[rad/s]	0	
q_5	[rad]	5.0615	7.0686
$\dot{q}_5$	[rad/s]	0	

CHAPTER 4

Results

4.1. Movement of upper limb in sagittal plane

Some of the results from performed simulations can be seen in Figs. 4.1, 4.2 and 4.3. Variation of angular orientations, angular velocities and control moments at the two joints are shown for three different cost functions defined by non-zero α_{cc}, α_{ct} and α_{qj}. Results for α_{qa} closely match those for α_{qj}. A sample movement pattern ($\alpha_{cc} = 1$ solution) can be seen in Fig. 4.4, which shows the arm positions for every second time station during the movement.

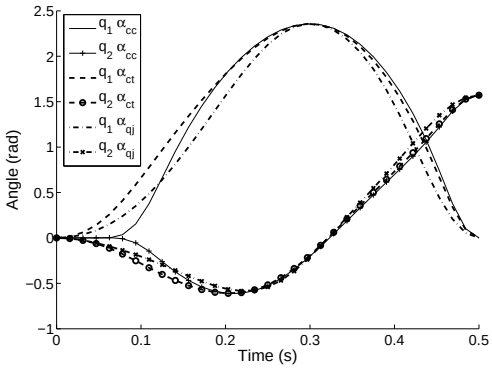

Figure 4.1: Variation of angles with time for three different cost functions

Five cost terms evaluated for the obtained solutions are given in Table 4.1; the different minimization functions are indicated by their non-zero α coefficients.

The colinearities between the full displacement vectors Q of the obtained solutions calculated according to Eq. (3.4) are shown in Table 4.2.

It was noted that other locally optimal solutions could be found for the case $\alpha_{cc} = 1$, if the initial guess to a solution was modified, Eriksson (2005). Further, a test with $\alpha_{cc} = 0.5$ and $\alpha_{qj} = 0.5 \cdot 10^{-5}$ gave a solution with $\Pi_{cc} = 17.6$ N^{2}m^{2}s, $\Pi_{ct} = 1241.5$ N^{2}m^2/s $\Pi_{qj} = 8.56 \cdot 10^5$ rad^2/s^5, $\Pi_{qa} = 4.78 \cdot 10^3$ rad^2/s^3, and $\Pi_{qv} = 31.3$ rad^2/s.

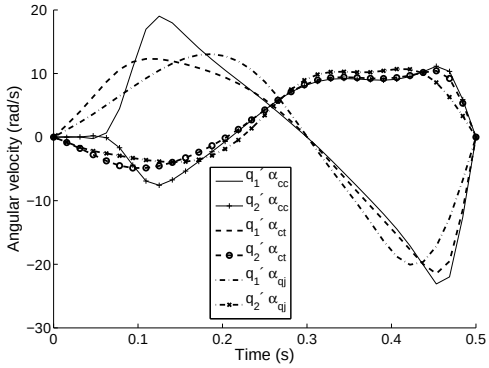

Figure 4.2: Variation of angular velocities with time for three different cost functions

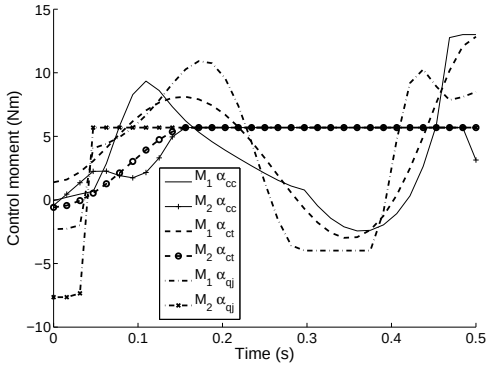

Figure 4.3: Variation of control moments with time for three different cost functions

The same movement was analyzed next but with different total movement durations T. Fig. 4.5 shows the variation of control force cost with increasing time. The solutions essentially showed waiting states before starting the same movement if $T \geq 0.65$ seconds. Similar conclusions were reached for other cost criteria.

Increasing the number of N_k resulted in oscillating behavior of control forces, as seen in Fig. 4.6 where three values of N_k (17,21,33) were used. Decreasing the number of N_k number did not have major effect.

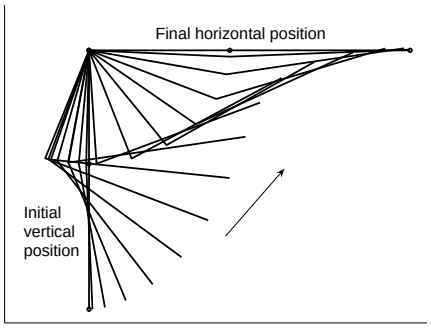

Figure 4.4: A sample movement pattern

Table 4.1: Evaluation of the different cost terms for solutions from different minimization criteria

Min. crit.	Cost term Π_{cc}, Eq. (2.21)	Π_{ct}, Eq. (2.23)	Π_{qj}, Eq. (2.25)	Π_{qa}, Eq. (2.26)	Π_{qv}, Eq. (2.27)
α_{cc}	13.2	3553	$2.57 \cdot 10^7$	$17.5 \cdot 10^3$	45.9
α_{ct}	14.3	1753	$1.10 \cdot 10^7$	$11.0 \cdot 10^3$	40.2
α_{qj}	18.9	10106	$2.89 \cdot 10^6$	$8.4 \cdot 10^3$	40.5
α_{qa}	18.6	8305	$3.64 \cdot 10^6$	$8.2 \cdot 10^3$	38.4
α_{qv}	19.4	10887	$4.50 \cdot 10^7$	$13.7 \cdot 10^3$	31.9
	[N^2m^2s]	[N^2m^2/s]	[rad^2/s^5]	[rad^2/s^3]	[rad^2/s]

Table 4.2: Evaluation of colinearites for Q vectors for five different minimization criteria

C_{ij}	α_{cc}	α_{ct}	α_{qj}	α_{qa}	α_{qv}
α_{cc}	1.0000	0.9675	0.9471	0.9462	0.9226
α_{ct}	0.9675	1.0000	0.9709	0.9790	0.9650
α_{qj}	0.9471	0.9709	1.0000	0.9982	0.9420
α_{qa}	0.9462	0.9790	0.9982	1.0000	0.9555
α_{qv}	0.9226	0.9650	0.9420	0.9555	1.0000

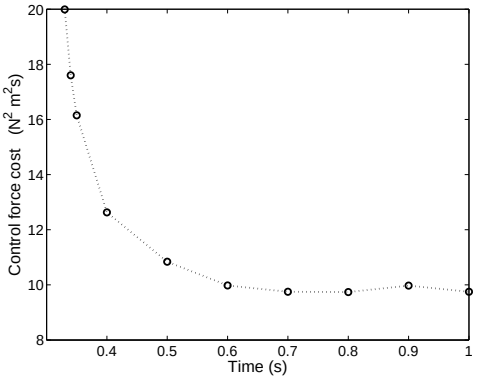

Figure 4.5: Effects of change in total time

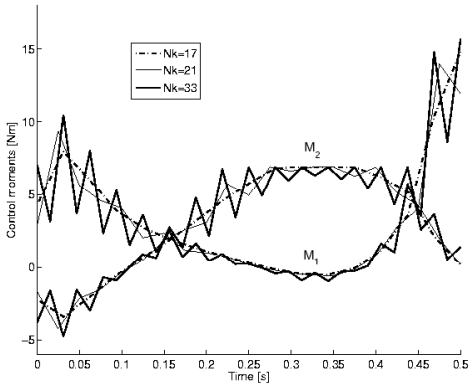

Figure 4.6: Effects of changing number of N_k, N_t is kept constant at 16

4.2. Tensions in muscles

Using muscle tensions as controls, the contribution of the involved muscles can be seen in Figs. 4.7 and 4.8. Fig. 4.7 corresponds to the minimization of squared muscle tensions, $\alpha_{cc} = 1$, whereas Fig. 4.8 corresponds to the minimization of squared rates of change of muscle tensions, $\alpha_{ct} = 1$.

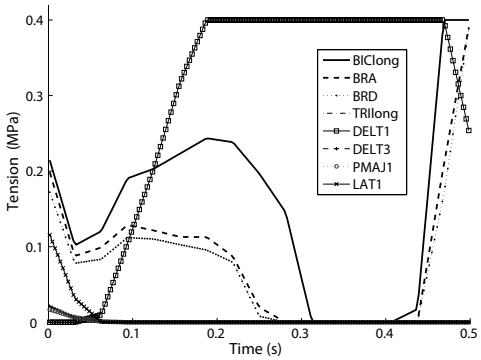

Figure 4.7: Contribution from individual muscles evaluated for $\alpha_{cc} = 1$

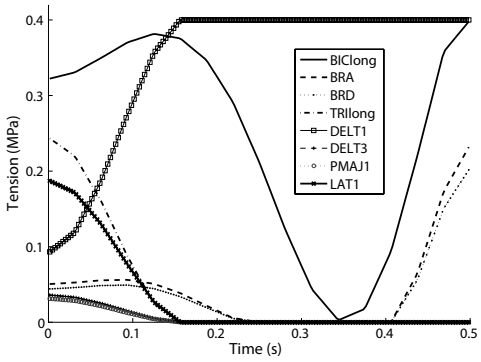

Figure 4.8: Contribution from individual muscles evaluated for $\alpha_{ct} = 1$

Biceps long head and deltoid anterior muscles were seen to play the major roles in both cases, although the action of biceps was more prominient for minimization with α_{ct} compared to that with α_{cc} criterion.

4.3. Movement of upper limb in horizontal plane

Trajectories of the lower arm end point for solutions based on three different minimization criteria (α_{cc}, α_{ct} and α_{qj}) can be seen in Figs. 4.9 and 4.10.

The velocity of the end point for the three different criteria can be seen in Fig. 4.11.

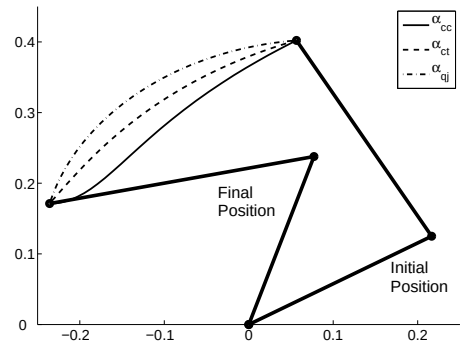

Figure 4.9: Trajectory of the wrist (Small movement)

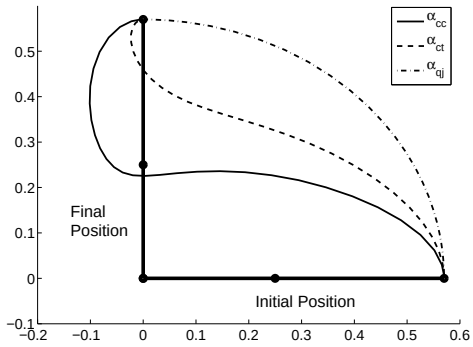

Figure 4.10: Trajectory of the wrist (Large movement)

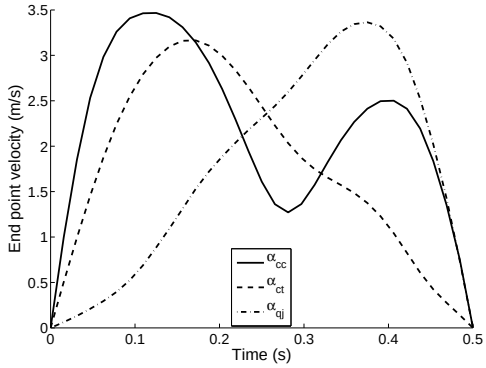

Figure 4.11: Velocity of the wrist (Large movement)

4.4. Vertical jumping

The results from high jump simulations performed for durations $T = 0.2$ and $T = 0.4$ seconds can be seen in Figs. 4.12 and 4.13. A sample movement pattern can be seen in Fig. 4.14.

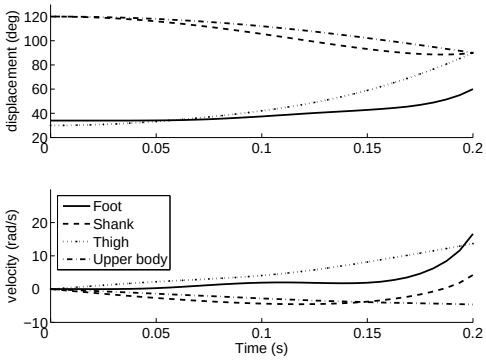

Figure 4.12: High Jump 0.2 s

From the angular velocities of the segments at the final state, the upward velocity of the centre of mass of the body was calculated to be 1.45 m/s for 0.2 s jump, while it was 3.1 m/s for 0.4 s duration jump. The heights reached were, thereby, about 11 and 50 cms respectively.

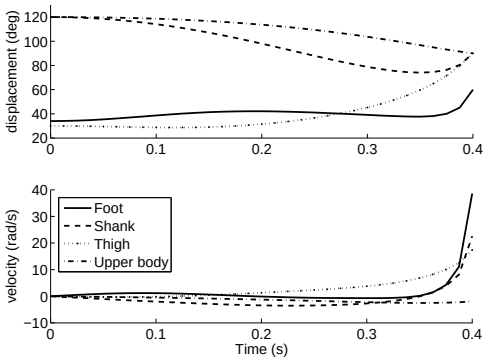

Figure 4.13: High Jump 0.4 s

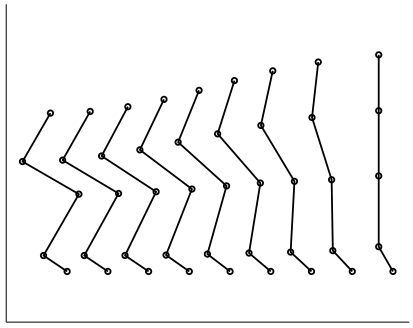

Figure 4.14: High Jump pattern

4.5. Walking/Stepping

The results from gait simulations are shown in Figs. 4.15 and 4.16. Experimental results from Gutierrez (2003) are included for comparision.

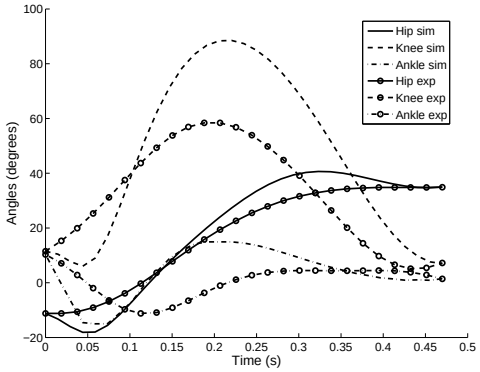

Figure 4.15: Gait simulation - a single step, sim - simulation, exp - experimental

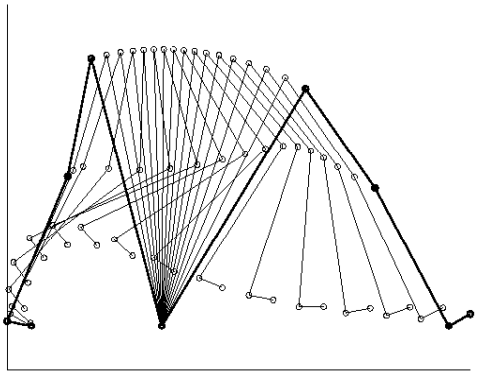

Figure 4.16: Gait pattern - a single step

For analysis of swing phase alone, variation in hip, knee and ankle angles are shown in Fig. 4.17 and the pattern of movement in Fig. 4.18.

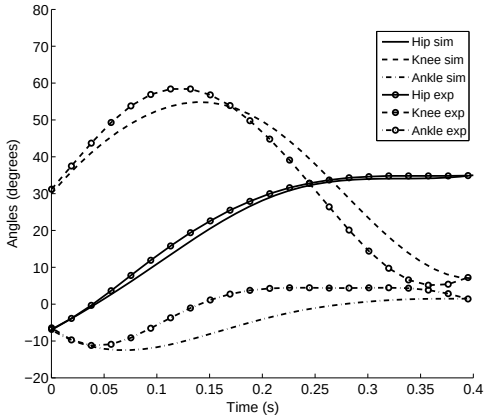

Figure 4.17: Gait simulation - swing phase, sim - simulation, exp - experimental

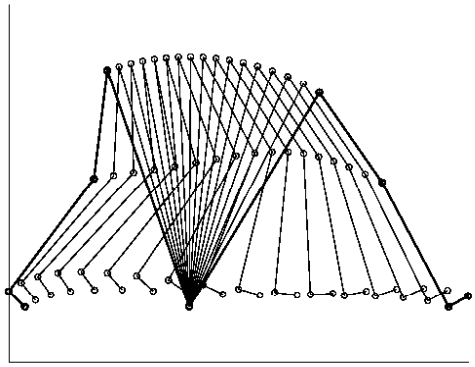

Figure 4.18: Gait pattern - swing phase

4.6. Weightlifting

Some of the results from weightlifting simulations can be seen in Figs. 4.19 and 4.20.

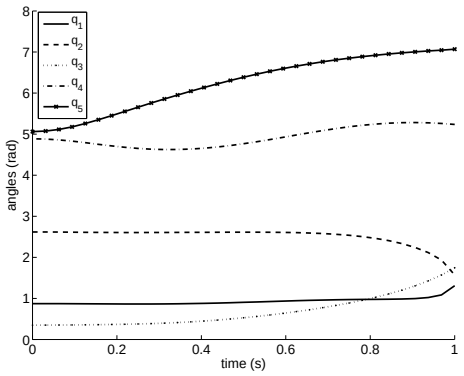

Figure 4.19: Weightlifting - segmental angles

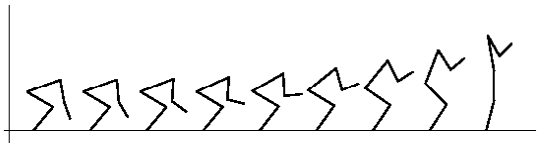

Figure 4.20: Weightlifting pattern

CHAPTER 5

Discussion

The main objective of this study was to compare the effects of different optimization criteria in modelling the dynamics of several common human movements. Performed simulations and obtained results indicate that the developed viewpoint and algorithm are efficient in the study of complex but primarily moderate sized forward dynamics problems. Different criteria for optimal movements can be easily introduced. Also, restrictions in form of linear and nonlinear constraints can be specified to give an improved description of human movements.

The results can be analyzed from both numerical and biomechanical point of views, though the accuracy of the results should be considered in the light of both assumptions and simplifications made. The proposed method and the developed algorithm can be used for more advanced biomechanical studies with incorporation of muscle mechanics and additional pysiological/anatomical properties. Possibility also exists for applications in other fields of engineering, (Eriksson and Tibert 2006).

It is obvious from the results that the optimization criterion used significantly affects the obtained solution. There is much discussion in literature on whether kinematic or kinetic optimization criteria are more suitable in predicting human movements.

For movements in vertical plane, Table 4.1 shows several interesting results, one being that for creating the smoothest solution (using $\alpha_{qj} = 1$), the magnitudes of the control forces are higher (around 15 to 20%) than those needed in $\alpha_{cc} = 1$ and $\alpha_{ct} = 1$ criteria solutions, cf. Eq. (2.22). Table 4.2 shows that α_{ct} and α_{qj} solutions are similar. This is expected, as force is proportional to acceleration, so rate of change in force can be expected to have close relation to jerk which is the rate of change of acceleration. Carrying out a desired movement in lesser time can be expected to demand more effort. This is precisely what is observed from Fig. 4.5, but it is noted that the algorithm will show a waiting state before the movement if the time is longer than the optimal. Minimum time has been used as optimization criterion in studies of human movements, (Pandy et al. 1995). The result shows that in this example, there exists an optimal duration of movement.

Force distribution among muscles deals with the issue of redundancy as more muscles than strictly needed are available. Physiological cross-sectional areas of muscles and moment arms are the contributing factors for force distribution among muscles. Criteria based on the control components are able to decide the force distribution among the muscles, but those based on the state variables, such as the jerk criterion, are not

able to do so. A criterion essentially minimizing jerk ($\alpha_{qj} \neq 0$) can, however, be accompanied by a small value of α_{cc} to resolve this computational ill-posedness.

The movements observed are upper arm flexion/extension at the shoulder joint and lower arm flexion/extension at the elbow joint. Biceps brachii, brachialis and brachioradialis are the major muscles flexing the elbow joint while triceps brachii acts as the extensor at the elbow joint, (Palastanga et al. 2002). The main muscles flexing the arm at the shoulder joint are anterior deltoid and biceps brachii, while those extending the arm are triceps, posterior deltoid, pectoralis major and latissimus dorsi, (Palastanga et al. 2002). The high levels of activity seen in biceps long and deltoid anterior (Figs. 4.7 and 4.8) match the expected behaviour.

It should be noted that in the physiological situation the moment arms of muscles change with the orientation of the segments and hence with time. But for simplicity, constant averaged values were used for the simulations. For more accurate results, change in moment arms with arm configuration must be accounted for and this is left as future work. Future work should also focus on the activation dynamics of muscles, as the present examples allow immediate regulation of forces, within stated limiting values.

For movements in the horizontal plane, slightly curved trajectories were obtained for smaller movements for the three simulation criteria used, Fig. 4.9. On the other hand, for larger movements, the control force criterion gives strongly curved paths while jerk cost gives a circular path with elbow angle remaining unchanged, Fig. 4.10. Regarding velocity profile, results from moment rate and jerk criteria match single peak bell shaped velocity profile (Fig. 4.11) described in previous studies, (Flash and Hogan 1985; Uno et al. 1989).

The analysis of high jump has been simplified to a large extent. The optimization criterion used in this setting was minimization of rate of moments, as this fitted the setting of the developed algorithm. Moments at the joints are created by muscles, so it seems reasonable to assume minimal moment change as optimization criterion, as a simple consideration of the delays in muscular force productions.

A simulated jump height of 33 cm has been reported in Pandy et al. (1990), who used maximum height reached by the centre of mass of the body as optimal control performance criterion. But the results obtained here show large variation in jump height and this can be attributed to simplifications made in the model. It is also noted that the present optimization method sees this problem in a very different manner than other criteria such as maximization of the jump height and velocity. Therefore, the two views should be seen as complementary rather than replacements of each other.

For gait simulation, handling of the double support phase presents some difficulties as constraining the toe position for a certain duration introduces additional nonlinear equality equations that have to be fulfilled. Using two nonlinear inequality constraints instead of one equality constraint is numerically stable. This also shows the possibility for specifying complex boundary conditions in the algorithm. Longer step length can be attributed to the simplification made by representing the stance leg with a single

straight segment. This also gives too high lift of the heel in the initial phase and excessive knee flexion, Fig. 4.16.

Gait simulation for a single step shows excessive knee flexion, but that the for swing phase alone gives good results. Results from weighlifting also match with those from Chang et al. (2001). Different cost criteria were attempted for both gait and weightlifting models, but the criterion related to minimization of rate of change of control forces/torques (nonzero α_{ct}) seemed to produce more reliable results in both cases.

The values of N_k and N_t affect the speed of calculation as these directly contribute to the number of unknown variables. Choosing too small values do not properly describe the dynamics of the system, whereas too high values demand higher computational cost. Trial and error approach was taken to ensure proper combination. In addition, study of variations of N_k with chosen N_t, Fig. 4.6, shows that the discretization points for controls must be less than or preferably coincident to those for state variables.

The calculation time is an important parameter. With most problems, it was of the order of few minutes. In some cases the iterations diverged instead of converging to an optimal point. The remedy used was changing the initial guess and running the simulations again. Often, after slight modifications, the algorithm could be used for evolution problem, which is represented by the initial value differential equations instead of the boundary value differential equations mainly discussed here, (Eriksson 2005, 2007). Using the evolution solution as the initial guess is an attractive alternative.

As discussed previously, trajectory planning is a key area in robotics. The proposed method is a viable option to study such problems. With appropriate modifications in the algorithm, other optimization criteria can be introduced. It should be stated that the quadratic forms of the used criteria enable easier differentiation to obtain the gradients. Other optimization criteria (for example, Cartesian jerk instead of angular jerk criterion) may introduce nonlinearities, but can still be used with proper modifications in the algorithm.

Comparision of different optimization criteria (in case of the larger models) was done visually. Though not shown, results obtained from optimization with π_{cc} criterion were markedly different from those from π_{ct} criterion for the weightlifting model, unless extensive constraints were used. With large number of variables and equations, the solution space is big and several possible solutions can exist. Constraints are often required to initially reduce the solution space and arrive at a feasible solution.

Extensive simplifications and assumptions used and lack of representation of real physiological behaviour imply that it is hard to draw definite biomechanical conclusions from the results. In most models the final conditions only specify displacements, as final velocities can be obtained only with experimental studies. Using more boundary conditions can be expected to give more reliable results. Nevertheless, results obtained indicate the possiblity of using the present method to solve wide classes of dynamic problems.

CHAPTER 6

Conclusions and Future work

Study of the forward dynamic models of several common human activities has yielded interesting results, in addition to verifying the usefulness of the developed algorithm. Results show that the method, based on temporal discretization followed by optimization, can successfully solve small to medium scale problems of varying complexities. The number of unknowns in the models typically vary between 100-1000 and similar numbers of equality and non-equality constraints exist. The algorithm is deemed suitable for analysis of similar applications in other fields, such as structural engineering and robotics.

Smoothness of resulting movement and economy in force usage were primary optimization criteria tested. From a physiological viewpoint, a criterion based on the rate of change of forces/torques seems better than other criteria tested, as it is close to the smoothness or jerk criterion, but is more well defined for redundant systems. Muscles can not act instantaneously, as there is a history and activaton dependence in force recruitment. To certain extent this problem is addressed by the α_{ct} criterion as it tends to make control forces change slowly.

Forward dynamics calculations are generally computationally expensive, but the algorithm converges reasonably efficiently with a good initial guess to a solution. Regarding convergence, it is believed impossible to strictly verify that an obtained solution is a global minimum for the formulated problem, (Nocedal and Wright 1999), but intelligent interpretation of results can probably always verify this.

One of the drawbacks of the stated formulation is the large numbers of equations and variables involved. Better ways to solve optimization problem may be needed for larger and more complex system. Several available optimization algorithms are being investigated, such as the method of moving asymptotes (MMA), (Svanberg 2002) and the 'SNOPT' optimization algorithm in its Comsol Script implementation (COMSOL AB, Stockholm).

Future work can be related to two different aspects of the models: mathematical and biomechanical. From the mathematical point of view, focus can be put on the following points:

- An important aspect is how to handle the very sparse matrices more effectively. This can considerably speed up the calculations.
- More advanced optimization algorithms may be necessary for larger problems.

- Handling of constraints such as complex nonlinear constraints and specifying a guess to initiate the solution process can be a subject of further analysis.
- Although not being of particular concern in present models, distinguishing between global and local optimal solutions is a problem that can be encountered when dealing with more complex models.
- Alternative ways of formulation to point collocation include Galerkin method for the weak formulation of the equations, (Zienkiewicz and Taylor 2000; Cook et al. 2002).

To make the models more realiable from the biomechanical point of view, the following factors can be considered:

- More anatomical and physiological aspects should be incorporated, such as limits on maximum and minimum joint moments or muscles forces and accurate information about moment arms and cross-sectional areas of muscles as functions of configuration.
- Muscle activation dynamics deals with mechanisms behind the force production in muscles (Pandy 2001; Ackermann and Schiehlen 2006). This can be incorporated in the models by using muscle activation levels as controls. This will present further computational challenge as controls then enter in nonlinear forms.
- The primary aim of this study was to compare results for different optimization criteria, rather than with experimental results. Still, carrying out experimental studies to compare the results from the simulations is an important future step.
- It is not entirely known which cost fuction is appropriate in which movement situation; a combination of various cost criteria may have to be tested to ensure accurate description of a movement.
- Studies on human movements seem to agree that a movement is produced through a planning process and a real-time feedback criterion. This study has only considered the planning phase, but the performance phase is well worthy of further analysis.

In conclusion, it can be said that human movements are complex activities and in order to model them, great simplifications are often necessary. In this study, the body parts have been modelled as rigid segments and the movements of these segments have been studied from a purely mechanical point of view, with neural control completely ignored. In spite of these shortcomings, the present method provides a simple way to increase the understanding of human movement strategies and provides several meaningful conclusions.

Bibliography

W. Abend, E. Bizzi, and P. Morasso. Human arm trajectory formation. *Brain*, 105:331–348, 1982.

M. Ackermann and W. Schiehlen. Dynamic analysis of human gait disorder and metabolical cost estimation. *Arch. Appl. Mech*, 75:569–594, 2006.

F. C. Anderson and M. G. Pandy. Dynamic optimization of human walking. *J. Biomech. Eng.*, 123:381–390, 2001.

M. Armand, J. P. Huissoon, and A. E. Patla. Formation and control of optimal trajectory in human multijoint arm movement. *IEEE Trans. on Rehab. Eng.*, 6:43–52, 1998.

R. Beauwens. Iterative solution methods. *Appl. Num. Math.*, 51:437–450, 2004.

J. T. Betts and W. P. Huffman. Application of sparse nonlinear programming to trajectory optimization. *Journal of Guidance, Control and Dynamics*, 15:981–985, 1992.

M. G. Calkin. *Lagrangian and Hamiltonian mechanics*. World Scientific, 1996.

D. B. Chaffin and G. B. J. Andersson. *Occupational Biomechanics*. John Wiley & Sons, Inc., USA, 1991.

C. Chang, D. R. Brown, D. S. Bloswick, and S. M. Hsiang. Biomechanical simulation of manual lifting using spacetime optimization. *J. Biomech.*, 34:527–532, 2001.

H. Chen and T. Lu. Comparisions of the joint moments between leading and trailing limb in young adults when stepping over obstacles. *Gait and Posture*, 23:69–77, 2006.

L. Chou and L. F. Draganich. Stepping over an obstacle increases the motions and moments of the joints of the trailing limb in young adults. *J. Biomech.*, 30:331–337, 1997.

R. D. Cook, D. S. Malkus, M. E. Plesha, and R. J. Witt. *Concepts and applications of finite element analysis*. Wiley, 4th edition, 2002.

S. L. Delp and J. P. Loan. A graphic-based software to develop and analyze models of musculoskeletal structures. *Comput. Biol. Med.*, 25:21–34, 1995.

J. Dul, M. A. Townsend, R. Shiavi, and G. E. Johnson. Muscular synergism — I. On criteria for load sharing between synergistic muscles. *J. Biomech.*, 17:663–673, 1984.

P. J. Enright and B. A. Conway. Optimal finite thrust spacecraft trajectories using collocation and nonlinear programming. *Journal of Guidance, Control and Dynamics*, 14:981–985, 1991.

A. Eriksson. Analysis methodology based on temporal FEM for bio-mechanical simulations. In M. Ursino, C. A. Brebbia, G. Pontrelli, and E. Magosso, editors, *Modelling in Medicine and Biology VI*, Southampton, 2005. WIT Press.

A. Eriksson. Temporal finite elements for target control dynamics of mechanisms. *Comp. Struct.*, 85:1399–1408, 2007.

A. Eriksson and A. G. Tibert. Redundant and force-differentiated systems in engineering and nature. *Comput. Methods Appl. Mech. Engrg.*, 195:5437–5453, 2006.

T. Flash and N. Hogan. The coordination of arm movements: an experimentally confirmed mathematical model. *J. Neurosci.*, 5:1688–1703, 1985.

H. Flashner, A. Beuter, and A. Arabyan. Modeling of control and learning in a stepping motion. *Biol. Cybern.*, 55:387–396, 1987.

Y. C. Fung. *Biomechanics: mechanical properties of living tissues*. Springer, New York, second edition, 1993.

B. A. Garner and M. G. Pandy. Musculoskeletal model of the upper limb based on the visible human male dataset. *Comp. Meth. Biomech. Biomed. Eng.*, 4:93–126, 2001.

W. Goldsmith. Biomechanics of solids. In S. A. Berger, W. Goldsmith, and E. R. Lewis, editors, *Introduction to bioengineering*, pages 1–99. Oxford University Press, New York, 1996.

E. M. Gutierrez. *Gait Strategy in Myelomeningocele: Movements, Mechanics and Methods*. Dr. thesis, Karolinska Institute, Stockholm, 2003.

J. Hamill and W. S. Selbie. Three-dimensional kinetics. In D. G. E. Robertson, G. E. Caldwell, J. Hamill, G. Kamen, and S. N. Whittlesey, editors, *Research Methods in Biomechanics*, pages 145–160. Human Kinetics, USA, 2004.

C. R. Hargraves and S. W. Paris. Direct trajectory optimization using nonlinear programming and collocation. *Journal of Guidance, Control and Dynamics*, 10:338–342, 1987.

S. Heintz and E. Gutierrez-Farewik. Static optimization of muscle forces during gait in comparision to emg-to-force processing approach. *Gait and Posture*, 26:279–288, 2007.

S. Heintz, E. Gutierrez-Farewik, and A. Eriksson. Evaluation of load-sharing and load capacity in force-limited muscle systems. *Comp. Meth. Biomech. Biomed. Eng.*, 2006. (submitted).

K. R. S. Holzbaur, W. M. Murray, and S. L. Delp. A model of the upper extremity for simulating musculoskeletal surgery and analyzing neuromuscular control. *Annals Biomed. Eng.*, 33: 829–840, 2005.

S. M. Hsiang, C. Chang, and R. W. McGorry. Development of a set of equations describing joint trajectories during para-sagittal lifting. *J. Biomech.*, 32:871–876, 1999.

R. Johansson and M. Magnusson. Optimal coordination and control of posture and locomotion. *Math. Biosciences*, 103:203–244, 1991.

M. L. Kaplan and J. H. Heegaard. Predictive algorithms for neuromuscular control of human locomotion. *J. Biomech.*, 34:1077–1083, 2001.

M. L. Kaplan and J. H. Heegaard. Second-order optimal control algorithm for complex systems. *Int. J. Numer. Meth. Eng.*, 53:2043–2060, 2002.

J. M. Knudsen and P. G. Hjorth. *Elements of Newtonian mechanics including nonlinear dynamics*. Springer, Berlin, second edition, 1996.

S. L. Lehman, R. Kram, and C. T. Farley. Locomotion and muscle biomechanics. In S. A. Berger, W. Goldsmith, and E. R. Lewis, editors, *Introduction to Bioengineering*, pages 387–415. Oxford University Press, New York, 1996.

M. Lesser. *The analysis of complex nonlinear mechanical systems: a computer algebra assisted approach*. World Scientific, Singapore, 1995.

S. Macfarlane and E. A. Croft. Jerk-bounded manipulator trajectory planning: design for real time applications. *IEEE Transactions on robotics and automation*, 19:42–51, 2003.

L. L. Menegaldo, A. T. Fleury, and H. I. Weber. Biomechanical modeling and optimal control of human posture. *J. Biomech.*, 36:1701–1712, 2003.

P. Morasso. Spatial control of arm movements. *Exp. Brain Res.*, 42:223–227, 1981.

S. G. Nash and A. Sofer. *Linear and Nonlinear Programming*. McGraw-Hill, Singapore, 1996.

J. Nocedal and S. J. Wright. *Numerical optimization*. Springer, 1999.

R. Nuzzo. Computational biomechanics: Making strides towards patient care. *Biomedical Computation Review, Winter 2006/07*, pages 10–19, 2006.

K. Ohta, M. M. Svinin, Z. Luo, S. Hosoe, and R. Laboissiere. Optimal trajectory formation of constrained human arm reaching movements. *Biol. Cybern.*, 91:23–36, 2004.

S. Onyshko and D. A. Winter. A mathematical model for the dynamics of human locomotion. *J. Biomech.*, 13:361–368, 1980.

N. Palastanga, D. Field, and R. Soames. *Anatomy and Human Movement*. Butterworth Heinemann, USA, 2002.

M. G. Pandy. Computer modelling and simulation of human movement. *Annu. Rev. Biomed. Eng.*, 3:245–273, 2001.

M. G. Pandy and M. Berme. A numerical method for simulating the dynamics of human walking. *J. Biomech.*, 21:1043–1051, 1988.

M. G. Pandy, B. A. Garner, and F. C. Anderson. Optimal control of non-ballistic muscular movements: A constraint-based performance criterion for rising from a chair. *Journal of Biomechanical Engineering*, 117:15–26, 1995.

M. G. Pandy, F. E. Zajac, E. Sim, and W. S. Levine. An optimal control model for maximum-height human jumping. *J. Biomech.*, 23:1185–1198, 1990.

S. J. Piazza and S. L. Delp. The influence of muscles on knee flexion during the swing phase of gait. *J. Biomech.*, 29:723–733, 1996.

L. Ren, R. K. Jones, and D. Howard. Predictive modelling of human walking over a complete gait cycle. *J. Biomech.*, 40:1567–1574, 2007.

W. S. Selbie and G. E. Caldwell. A simulation study of vertical jumping from different starting postures. *J. Biomech.*, 29:1137–1146, 1996.

T. Spägele, A. Kistner, and A. Gollhofer. Modelling, simulation and optimisation of a human vertical jump. *J. Biomech.*, 32:521–530, 1999.

M. W. Spong, S. Hutchinson, and M. Vidyasagar. *Robot Modelling and Control*. John Wiley & Sons, USA, 2006.

M. Stelzer and O. von Stryk. Efficient forward dynamics simulation and optimization of human body dynamics. *J. Appl. Math. and Mech., ZAMM*, 1:1–1, 2003.

D. H. Sutherland, K. R. Kaufman, and J. R. Moitoza. Kinematics of normal human walking. In J. Rose and J. G. Gamble, editors, *Human Walking*, pages 23–44. Williams & Wilkins, USA, 1994.

K. Svanberg. A class of globally convergent optimization methods based on conservative convex seperable approximations. *SIAM J. Optim.*, 12:555–573, 2002.

Y. Uno, M. Kawato, and R. Suzuki. Formation and control of optimal trajectory in human multijoint arm movement. *Biol. Cybern.*, 61:89–101, 1989.

D. A. Winter. *Biomechanics and motor control of human movement*. Wiley, Hoboken, NJ, USA, 3rd edition, 2005.

O. C. Zienkiewicz and R. L. Taylor. *The finite element method. Volume 1: The basis*. Butterworth-Heinemann, Oxford, 5th edition, 2000.

APPENDIX A

Sequential Quadratic Programming

The basic idea of SQP is to model the nonlinear problem by a quadratic subproblem at each iterate and to define the search direction as the solution of this subproblem. An estimate of the Hessian of the Lagrangian is updated in each iteration using a BFGS method (Nash and Sofer 1996; Nocedal and Wright 1999).

The nonlinear problem to be solved is:

$$\begin{aligned} \text{mimimize} \quad & \Pi(\boldsymbol{z}) \quad \text{subject to} \\ & \boldsymbol{b}_1(\boldsymbol{z}) = 0 \\ & \boldsymbol{b}_2(\boldsymbol{z}) \leq 0 \end{aligned} \tag{A.1}$$

Lagrangian L is formed as:

$$L(\boldsymbol{z}, \boldsymbol{\lambda}) = \Pi(\boldsymbol{z}) + \boldsymbol{\lambda}^T \boldsymbol{b} \tag{A.2}$$

where $\boldsymbol{\lambda}$ are the Lagrange multipliers and $\boldsymbol{b}$ includes both $\boldsymbol{b}_1$ and $\boldsymbol{b}_2$. In SQP, the problem is then stated as:

$$\begin{aligned} \text{mimimize} \quad & \frac{1}{2} p^T H_k p + \nabla \Pi(\boldsymbol{z}_k)^T p \quad \text{subject to} \\ & \nabla \boldsymbol{b}_1(\boldsymbol{z}_k)^T p + \boldsymbol{b}_1(\boldsymbol{z}_k) = 0 \\ & \nabla \boldsymbol{b}_2(\boldsymbol{z}_k)^T p + \boldsymbol{b}_2(\boldsymbol{z}_k) \leq 0 \end{aligned} \tag{A.3}$$

where H_k denotes the Hessian of the Lagrangian and p is the search direction.

p at the current iterate k is used to find next solution as:

$$\boldsymbol{z}_{k+1} = \boldsymbol{z}_k + p_k \tag{A.4}$$

Acknowledgement

First of all, I would like to thank my supervisor Prof. Anders Eriksson for his help, guidance and understanding thoroughout the project.

In this time I got a chance to gain valuable knowledge in various fields of engineering and science. I thank all my teachers in the university for this opportunity.

I am also grateful towards everyone at the department, especially the members of Structural/Biomechanics group, for their friendship and for helping create pleasant working environment.

Finally, thanks to my parents, sisters and my little niece for their love and constant encouragement.

Review of Paper

This licentiate thesis includes a manuscript entitled:

Optimality in forward dynamics simulations
M. Kaphle and A. Eriksson 2007
Submitted to the *Journal of Biomechanics*

Some of the results in this thesis were presented in
19th Nordic Seminar on Computational Mechanics
Lund, 20-21 October, 2006.